Experimental and Numerical Test of Radial Internal Magnetic Spur Gear

Kafi Hannan Alhadi
Department of Mechanical Engineering, Institut Teknologi Sepuluh Nopembe

Agus Sigit Pramono
Department of Mechanical Engineering, Institut Teknologi Sepuluh Nopembe

https://doi.org/10.5109/7236867

出版情報：Evergreen. 11 (3), pp.2248-2256, 2024-09. Interdisciplinary Graduate School of Engineering Sciences, Kyushu University, Japan
バージョン：

Experimental and Numerical Test of Radial Internal Magnetic Spur Gear

Kafi Hannan Alhadi, Agus Sigit Pramono*
Department of Mechanical Engineering, Institut Teknologi Sepuluh Nopember, Surabaya, Indonesia

*Author to whom correspondence should be addressed:
E-mail: pramono@me.its.ac.id

(Received October 29, 2023: Revised June 7, 2024: Accepted June 21, 2024).

Abstract: Magnetic gears have the advantage of low noise compared to mechanical gears because there is no contact between solid materials. However, magnetic gear has the disadvantage of having a lower torque density than mechanical gear. For this reason, the study of efforts to increase torque density is an interesting topic for research. In this research, how to produce a larger torque at a constant magnetic volume by varying the number of poles and reducing the thickness of the magnet at a constant magnetic volume. In addition, the air gap is also varied, which corresponds to the tolerance in the manufacture of high-speed gear and low-speed gear on the internal magnetic gear. The research was conducted using 3D modeling and experiments**.** As a result of this research, it is known that the addition of the number of poles 2 to 4 poles on high-speed gear and 4 to 8 poles on low-speed gear with total volume magnet constant, will increase the maximum static torque value of 15.9% and 43%, respectively. Besides that, the air gap reduction with an interval of 0.2 mm will cause an increase in the maximum static torque value of 3.8% to 5.3%. A comparison between numerical and experimental results is also discussed in this study.

Keywords: internal magnetic spur gear; magnet; pole; air gap; torque

1. Introduction

Mechanical gears have many advantages in their use, both in large topologies and in small topologies such as robot prototyping[1] which is currently being developed for many sectors. However, that does not mean that there are no shortcomings in the application of mechanical gear. One of the shortcomings of mechanical gears arises because of the need for contact between the teeth of the drive and driven gears. Solid mechanical parts that have direct contact with each other will involve a lot of friction and really need a lubrication system[2–5]. If contact and rolling on the tooth surface occurs at high stress and occurs repeatedly, it can cause inherent wear, which can trigger gear failure. As a result of this, contact can also cause other losses such as wear on the gears, an increase in excess temperature due to friction that is repeated continuously, and noise from friction that occurs[6]. As we know, friction on metal will cause metal to wear out and affect the lifetime of the metal[7–10]. The existence of a system that involves friction between two materials requires the system to have adequate lubrication[3,8]. In addition, due to the absence of slippage when excessive torque occurs, the gears can experience severe damage. Several studies have been conducted to analyze friction and tribological properties[11,12], and also to develop an adequate lubrication system[13,14].

The use of materials that have magnetic properties has very broad benefits, both in the medical field[15], automotive equipment and machinery[16–20], nuclear fusion[21], biological science[22], and many other uses. Along with developing the use of magnets, research is also being carried out to obtain raw materials for magnets[23]. Magnetic gear has many advantages due to the absence of contact between the driving gear and the driven gear[24]. One type of magnetic gear that exists is the radial internal magnetic spur gear. Internal magnetic gear is claimed to have the ability to transmit higher torque when compared to external magnetic gear models[25]. In the process of developing this magnetic gear, it is necessary to continuously analyze the influencing variables to improve the ability of the magnetic gear to transmit torque. Analytical equations have been developed to model the magnetic field strength and torque resulting from coupled multipole cylinders[26]. Furthermore, there is a comparison of the analytical two-dimensional model and the finite element with experiments for the external magnetic gear model[27]. From this analysis, it was found that there was a 39% difference between the results of the two-dimensional analytical model and the finite element model with the experimental results.

A simple model of magnetic gear is external and internal magnetic gear. These two models are early models of magnetic gear before being developed into many new topologies of magnetic gear. Several previous studies have been conducted to analyze the performance of external magnetic gear[28–30]. From that research, it is known how the air gap and the number of poles influence the external magnetic gear's ability to transmit torque. Several researchers have developed a simple magnetic gear model into several new topologies. It aims to get a magnetic gear model that has better torque transmission capability. Many developments in the new magnetic gear topology started with a simple internal magnetic gear model. One of them is the coaxial magnetic gear model[31]. Several studies of analytical models, finite elements, and experiments have been carried out to analyze the performance of coaxial magnetic gears[32–36]. In addition to the coaxial model, there are also several other development models, such as transverse flux magnetic gear[37] and cycloidal magnetic gear[38]. From the development of the model, they obtained a better torque transmission capability on the magnetic gear.

Based on the direction of the magnetic flux in the magnetic gear, magnetic gear can be divided into magnetic gear with axial and radial flux directions. A Comparison of the performance of those two types of magnetic gear has been done before[39]. In the process of developing magnetic gears, it is analyzed how the performance of magnetic gears compares with mechanical gears[40]. From previous studies there are also reviews and state of the art to compare the performance of several existing magnetic gear models[41,42]. The use of wind turbines requires a transmission system and kinematics that can maximize the power generated[43]. Most of the uses of magnetic gears are applied to wind turbines. Several studies were conducted to analyze the performance of magnetic gears applied to wind turbines[44,45].

From several previous studies, it can be seen that the development of the current magnetic gear topology is a modification of the internal magnetic gear model. This study was conducted to provide an analysis related to the capabilities of a simple internal magnetic gear model, which is the forerunner of the current development of magnetic gear topology. This study will analyze the influence of the number of poles and the air gap with a constant total magnetic volume on the internal magnetic gear's ability to transmit torque. The three-dimensional finite element method using Ansys Maxwell and the experimental method used in this study. This study will also analyze how the results of the two methods compare. Thus, it is hoped that this research can provide information regarding the radial internal magnetic gear's ability to transmit torque with numerical finite element and experimental method which has not been extensively analyzed.

2. Methods

The research design using the finite element numerical method is used in this study to assist the analytical calculation process with very complex equations. The formulation of torque from the internal radial pair of a magnetic spur gear can be approached with the torque equation for the cycloidal magnetic gear type. Topologically, this cycloidal magnetic gear is identical to the internal magnetic gear. It is just that the cycloidal magnetic gear has components and movement patterns that are more complex when compared to the internal magnetic gear. Torque equations and magnetic fields in cycloidal magnetic gears that can be used as an approach to analyze torque in internal magnetic gears have been described in Jorgensen's research[38].

2.1 Finite Element Method

In this research, a simple internal magnetic gear model is formed that only consists of high-speed gear (driver) and low-speed gear (driven). This model does not involve the presence of a ferromagnetic pole piece as a link between the driver gear and driven gear, as in the coaxial magnetic gear model.

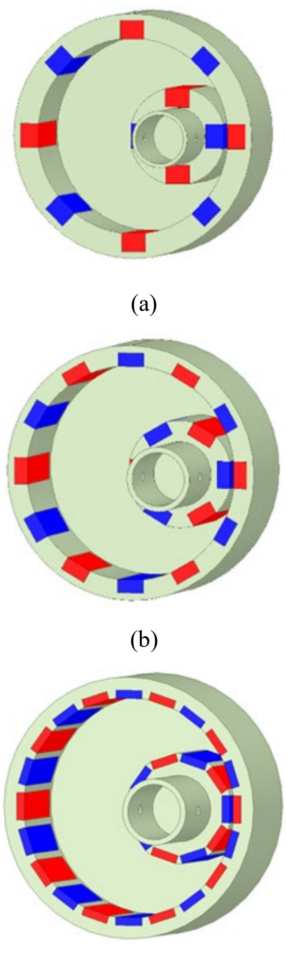

(a)

(b)

(c)

Fig. 1: Radial internal magnetic spur gear model (a) 4-8 pole; (b) 6-12 pole; (c) 10-20 pole

In this study, 3 variations of the number of poles were used: 4–8 poles, 6–12 poles, and 10–12 poles.

Each variation uses magnets of the same width and the same total volume of magnets. The determination of the number of poles is adjusted to the size of the neodymium N35 magnet available on the market. The availability of permanent magnet sizes in the market is a consideration for determining the number of poles in this study. Details related to the internal magnetic gear design are listed in Table 1.

Table 1. Magnetic gear model used

High-speed gear design	gear diameter (mm)	40
	shaft hole diameter (mm)	18.5
	width (mm)	30
Low-speed gear design	gear diameter (mm)	80
	shaft hole diameter (mm)	18.5
	width (mm)	30
Number of poles (HS *gear* - LS *gear*)	4-8 pole	magnet size 30x10x7,5 mm
	6-12 pole	magnet size 30x10x5 mm
	10-20 pole	magnet size 30x10x3 mm
Air gap	variation 1	1.6 mm
	variation 2	1.4 mm
	variation 3	1.2 mm

Magnetic gear modeling in this study uses PLA as a gear blank material and uses a rectangular N35 grade neodymium magnet. The material properties of these materials are listed in Table 2.

Table 2. PLA and magnetic material properties

NdFeb N35 Properties	
Remanence (T)	1,15
Relative permeability	1,09977
Mass density (kg/m^3)	7400
Curie Temperature (°C)	310
PLA Properties	
Density (g/cm^3)	1,3
Melting temperature (°C)	173
Tensile strength (MPa)	37
Elongation (%)	6
Flexural modulus (GPa)	4

After making the radial internal magnetic spur gear model, finite element analysis was carried out using the three-dimensional Ansys Maxwell Electromagnetic software with magnetostatic and transient analysis completed. The results of the modeling in the previous stage are continued by adjusting the mesh value in the magnetostatic analysis where the mesh size must converge. After the mesh refinement is done on the magnetostatic, the mesh in the transient analysis is connected so that it can use the results of the refinement mesh on the magnetostatic. Then some settings are made on the transient analysis to determine the density of the magnetic field (B) and the torque (T) generated by the magnet gear.

Analysis using the finite element method uses an approach related to the ideal magnetic strength distribution. where in reality we cannot get an ideal magnet that has the same distribution of magnetic strength on each side. Apart from that, the finite element method also does not represent the air gap which really corresponds to actual conditions. Some boundary conditions like that have the potential to produce quite significant differences in values between the finite element method and the experimental method. However, the finite element method would be much better if it could truly represent actual conditions.

2.2 Experimental Method

The experimental method was carried out in this study through a comparison of the numerical results. The experimental scheme can be seen in Fig. 2.

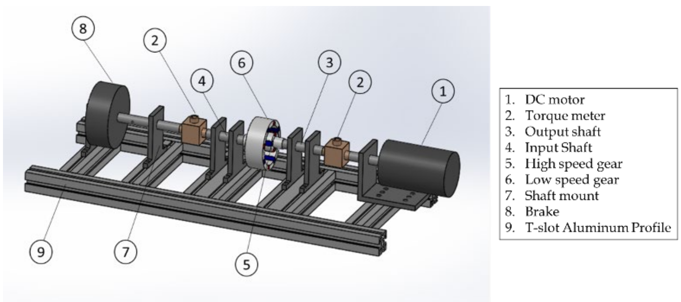

(a)

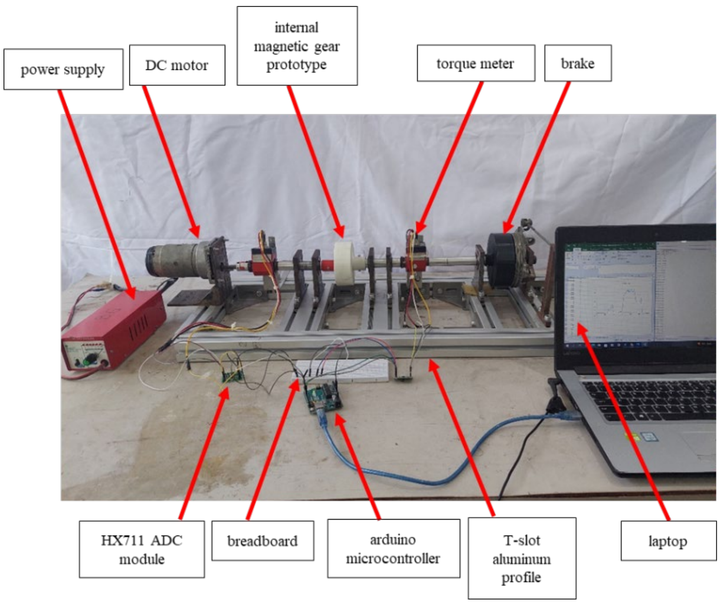

(b)

Fig. 2: Experimental scheme (a) 3D modeling; (b) assembly

This experiment uses torque meters, which are connected to the input shaft and the output shaft of the magnetic gear. The input shaft will get input rotation from the motor, and the output shaft will get the load from the connected brake. The motor is set to have a constant speed of 110 rpm. The experimental scheme of this study only focused on 10–20 pole pairs which adequate to validate all of the variation in this study. The sizes of the magnets in this study were adjusted to those on the market, and sizes were used so that each variation of the pole pair had the same total magnetic volume.

In this research, 2 types of experiments were carried out to observe static torque and dynamic torque. To analyze static torque, rotational input from a lever connected to the input shaft is used to rotate the magnetic gear transmission system. The output shaft is held in a stationary condition until losses occur from the magnetic pair in the driver and driven gear. Meanwhile, to analyze dynamic torque, rotational input from the motor is used to move the inout shaft and the output shaft is given a load gradually.

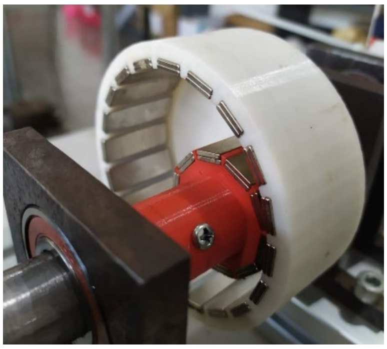

Fig. 3: Radial internal magnetic spur gear prototype

The radial internal magnetic spur gear prototype can be seen in Fig. 3. A feeler gauge is used to determine the air gap in the magnetic gear according to the specified variation. The torque analyzed in this study is the output torque generated by the magnetic gear. Before conducting the experiment, it is necessary to calibrate the torque meter. Torque meter calibration is carried out using a torque wrench as a reference for the torque value that will be read by the torque meter. Schematic and calibration results can be seen in Fig. 4.

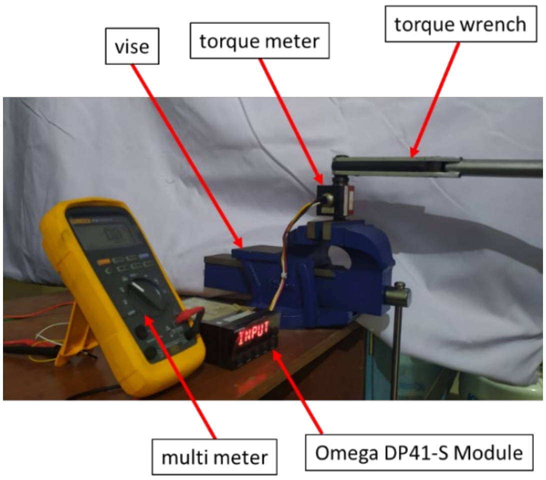

(a)

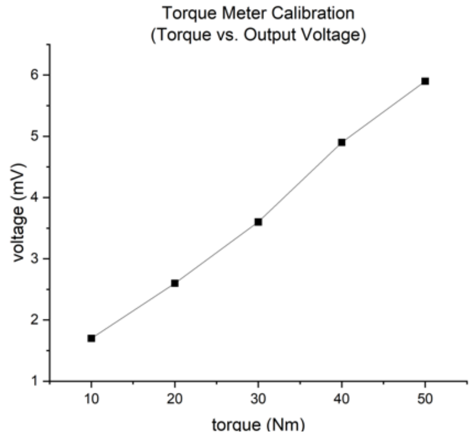

(b)

Fig. 4: Torque meter calibration (a) calibration scheme; (b) calibration result

During the calibration process, the torque meter is clamped in a vise. The torque meter is given a voltage input from the "DP41-S Omega" module of 10 volts. Furthermore, the torque meter is given a torque input using a torque wrench. From the torque wrench, it can be seen how much torque is given to the torque meter. The output voltage from the torque meter can be seen for each given torque input. The multimeter is used to observe the output voltage of the torque meter. This voltage output value can be used as verification against torque meter specifications. The output voltage value of the torque meter is in the form of analog data. In the experimental scheme, this analog data will be sent to the HX711 ADC module. This module will convert analog data into digital data. Digital data will be read through the Arduino microcontroller. Through the Arduino program, we can determine how much torque is read on the torque meter by inputting the calibration value into the program. This calibration constant will convert the ADC value into a torque value according to the input torque given during the calibration process. Before carrying out the experimental process, it is necessary to measure how straight the system that has been assembled is. The straightness measurement scheme can be seen in Fig. 5.

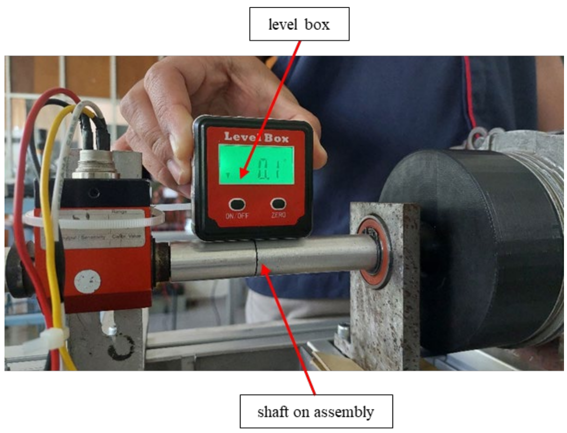

Fig. 5: Straightness measurement on assembly

The level box is used to measure the straightness of the assembly. Straightness in assembly is an important factor in analyzing torsion in experiments. Torque readings on the torque meter are very sensitive to the alignment of the assembly. The missing alignment will cause torque readings to be incorrect and the rotational motion of the assembly to be unbalanced. In this study, a fairly good alignment was obtained. Alignment in the assembly only has a slope of 0.1 degrees, according to the measurements in Fig. 5.

Real-time torque reading from magnetic gear using an Arduino microcontroller and HX711 ADC module. This experimental method was carried out to observe static and dynamic torque. Static torque is obtained by rotating the input shaft instead of using a motor. Meanwhile, dynamic torque is obtained by providing rotation on the input shaft using a motor. The output shaft is loaded through the brakes until a slip or loss interaction occurs on the magnetic gear. With such a scheme, the maximum torque of the magnetic gear will be known before the slip occurs.

3. Results and Discussion

3.1 Finite Element Results

There are 3 variations in the number of poles used in this study, namely variations with a number of 4–8 poles, 6–12 poles, and 10–20 poles. By varying the number of poles, it will be known how the number of poles influences the torque value that can be transmitted by the radial internal magnetic spur gear.

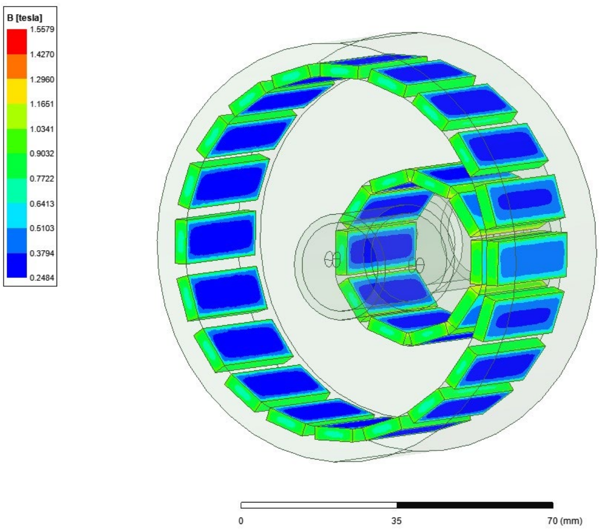

Fig. 6: Flux density in the magnetic pole pair

By using the finite element method, it can be seen how the flux density in the pole pair varies. In Figure 6, it can be seen that the magnets on the high-speed gear and low-speed gear that are paired will have a higher flux density than the magnets that are far apart or not paired with each other. With three-dimensional analysis, it will be seen that the flux distribution in the magnet is not uniform. The edge of the magnet will have a higher flux when compared to the center. This is because the edge has a relatively closer distance between the south pole and the north pole. The flux density will increase along with the smaller air gap in the pole pair. This will affect the torque generated from the magnetic gear.

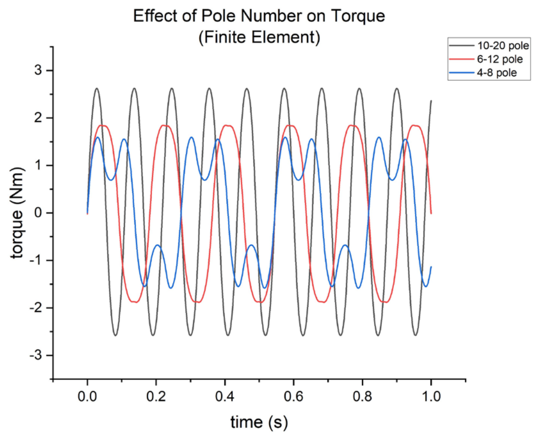

(a)

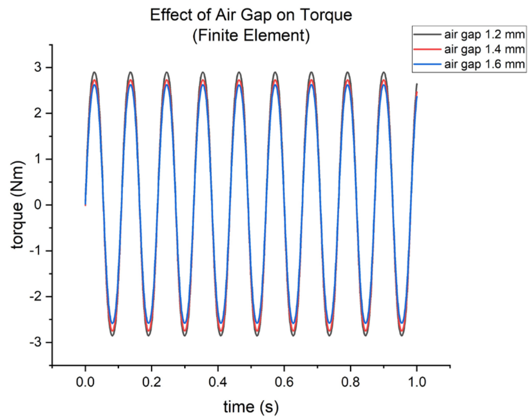

(b)

Fig. 7: (a) Effect of pole number on torque; (b) effect of air gap on torque (finite element)

In Figure 7(a) by running finite element method with static torque analysis, it can be seenthat the difference in the number of poles used will affect the torque value that can be transmitted by the radial internal magnetic spur gear. This can be seen from the maximum torque value that can be produced at each different pole pair and also from how the torque continuity is generated. By observing the maximum torque value, it will be found that as the number of poles used in the radial internal magnetic spur gear increases, the maximum torque value that can be transmitted will be greater. With the number of pole pairs 4–8, the maximum torque value that can be transmitted is 1.6 Nm, the number of pole pairs 6–12 can transmit a maximum torque of 1.85 Nm, and the number of pole pairs 10–20 can transmit a maximum torque of 2.6 Nm.

Meanwhile, how the air gap affects the resulting torque can be seen in Fig. 7(b). By observing the maximum torque value, it will be found that the smaller the air gap between the high-speed gear and low-speed gear, the greater the maximum torque value that can be transmitted.

With an air gap of 1.6 mm, the maximum torque value that can be transmitted is 2.63 Nm, an air gap of 1.4 mm can transmit a maximum torque of 2.73 Nm and an air gap of 1.2 mm can transmit a maximum torque of 2.9 Nm. The fluctuation of torque value from positive to negative is due to the static numerical method simulation scheme. This static numerical method simulation scheme will cause the magnetic pole encounter between the high-speed gear and low-speed gear to fluctuate between the same pole encounter and different pole encounters.

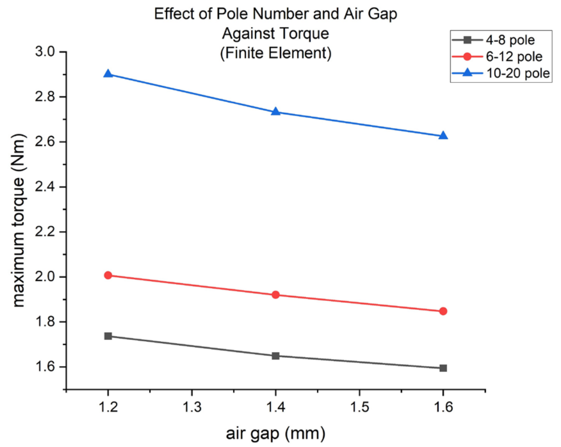

Fig. 8: Effect of pole number and air gap against torque (finite element)

Figure 8 shows that the addition of the number of poles from 2 to 4 in high-speed gear, and from 4 to 8 in low-speed gear will increase the maximum static torque value of 15.9% and 43%, respectively. In addition, it can be seen that the air gap reduction with an interval of 0.2 mm will cause an increase in the maximum static torque value of 3.8% to 5.3%. Based on the level of increase in the maximum torque value, it can be seen that the addition of the number of poles with an interval of 2 to 4 poles on high-speed gear and 4 to 8 poles on low-speed gear has a more significant effect than reducing the air gap with an interval of 0.2 mm.

3.2 Experimental Results

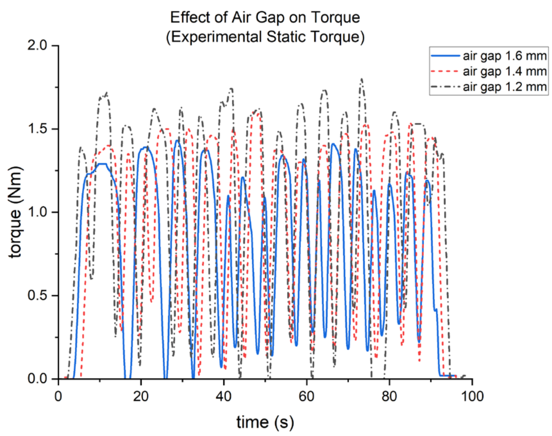

(a)

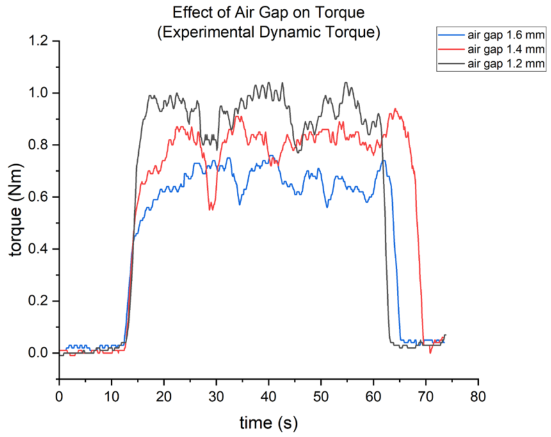

(b)

Fig. 9: Effect of air gap on torque (a) experimental static torque; (b) experimental dynamic torque

The other method used in this research is the experimental method. Figure 9(a) depicts how the radial internal magnetic spur gear generates static torque readings. By observing the maximum static torque value, it will be found that the smaller air gap used will cause the maximum static torque value that can be transmitted to be greater. With an air gap of 1.6 mm, the maximum static torque value that can be transmitted is 1.43 Nm. An air gap of 1.4 mm can transmit a maximum torque of 1.6 Nm, and an air gap of 1.2 mm can transmit a maximum torque of 1.8 Nm. With an air gap reduction interval of 0.2 mm, the maximum value of static torque increases from 11.8% to 12.5%.

Figure 9(b) shows how the dynamic torque readings are generated from a radial internal magnetic spur gear with a constant input speed of 110 rpm on a high-speed gear. In Figure 9(b) it can be seen that with an air gap of 1.6 mm, the maximum dynamic torque value that can be transmitted is 0.76 Nm, an air gap of 1.4 mm can transmit a maximum dynamic torque of 0.94 Nm, and an air gap of 1.2 mm can transmit a maximum dynamic torque of 1.04 Nm. With an air gap reduction interval of 0.2 mm, the maximum dynamic torque value increases from 10.6% to 23.7%. The phenomenon of slipping magnetic gear can be seen in the figure. This slip or loss interaction can be observed with a significant decrease in the dynamic torque value after reaching the maximum torque value.

3.3 Comparison Between Finite Element and Experimental Result

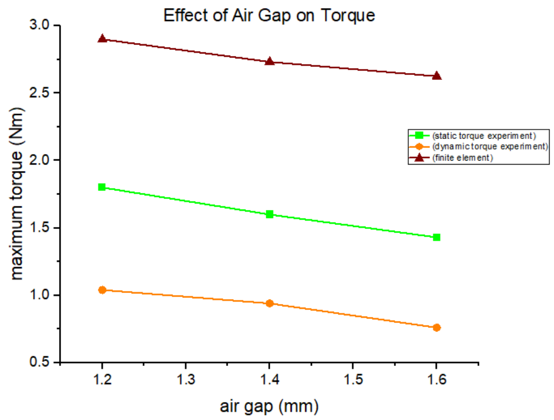

Fig. 10: Comparison between finite element and experimental result

Based on Figure 10, it can be seen that the radial internal magnetic spur gear's ability to transmit static and dynamic torque is significantly different. The difference in the maximum value of static torque and dynamic torque from the experimental results ranges from 70% to 88%. The difference arises because the observation of dynamic torque involves many moving components, where these components become variables that affect the magnetic gear's ability to transmit dynamic torque.

In Figure 10, it can also be seen that the static torque value of the finite element method and the experimental method have a very significant difference. The difference in the maximum value of static torque between simulation and experiment is between 61% and 83%. This difference is caused by the input of the permanent magnet strength value in the finite element method based on the general approach of neodymium magnet material properties with grade N35. In ideal circumstances, the magnetic strength input into the finite element method should be based on measurements taken with a Gauss Meter to measure the magnetic strength used in the experimental circuit. This research is limited to the existence of the Gauss Meter measuring instrument so that the magnetic strength at the input of the finite element method is only based on general material properties. In addition, the cause of the difference in results is the presence of a fairly large tolerance of the magnetic gear assembly geometry. The large tolerance of the magnetic gear geometry in this experiment will cause the existing air gap to not be constant for each pair of poles.

4. Conclusions

This study analyzes the ability of a simple internal magnetic gear model to transmit torque. The methods used in this research are finite element and experiment. From all methods, it is found that the smaller the air gap and the more of poles used, the greater the torque that can be transmitted by the radial internal magnetic spur gear. Based on finite element method we can see the addition of the number of poles from 2 to 4 in high-speed gear, and from 4 to 8 in low-speed gear will increase the maximum static torque value of 15.9% and 43%, respectively. In addition, it can be seen that the air gap reduction with an interval of 0.2 mm will cause an increase in the maximum static torque value of 3.8% to 5.3%. Meanwhile we can see from experimental results that air gap reduction with interval of 0.2 mm will cause the maximum value of static torque increases from 11.8% to 12.5%.

This research provides information indicating that the ability of magnetic gear to transmit static and dynamic torque is different. The difference in the maximum value of static torque and dynamic torque from the experimental results ranges from 70% to 88%. This is useful to illustrate that, in analyzing the ability of the magnetic gear, it is necessary to involve dynamic variables to get the true ability of the magnetic gear to transmit torque. This study also shows that in finite element modeling, it is necessary to provide values that correspond to what is in actual conditions to obtain the best approximation results; however, experimental geometry is an important variable when analyzing the ability of magnetic gears to transmit torque.

Acknowledgments

The authors would like to thank the Mechanical Engineering Department - Institut Teknologi Sepuluh Nopember, especially the Solid Mechanics Laboratory which has supported this research.

References

1) J. Nagpal, R. Lal, and R. Rana, "Novel robotic platform for affordable and customizable testing and prototyping," *Evergreen*, **10** (*1*) 454–462 (2023). doi:10.5109/6782148.
2) A.C. Opia, M.K.A. Hamid, S. Syahrullail, A.I. Ali, C.N. Johnson, I. Veza, M.I. Izmi, C.D.Z. Hilmi, and A.B. Abd Rahim, "Tribological behavior of organic anti-wear and friction reducing additive of zddp under sliding condition: synergism and antagonism effect," *Evergreen*, **9** (*2*) 246–253 (2022). doi:10.5109/4793628.
3) Y. Aiman, S. Syahrullail, H. Hafishah, and M.N. Musa, "Friction characteristic study on flat surface embedded with micro pit," *Evergreen*, **8** (*2*) 304–309 (2021). doi:10.5109/4480707.
4) K.S. Phad, and A. Hamilton, "Experimental investigation of friction coefficient and wear of sheet metals used for automobile chassis," *Evergreen*, **09** (*04*) 1067–1075 (2022). doi:10.5109/6625719
5) L.N. Patil, H.P. Khairnar, J.A. Hole, D.M. Mate, A. V. Dube, R.N. Panchal, and V.B. Hiwase, "An experimental investigation of wear particles emission and noise level from smart braking system," *Evergreen*, **9** (*3*) 711–720 (2022).

doi:10.5109/4843103

6) W. Emar, Z. Al-Omari, and T. Rawashdeh, "Slip-ring induction motor torque and current ripple minimization using bang-bang current control," *Evergreen*, **10** (*2*) 962–975 (2023). doi:10.5109/6792891.
7) A.K. Verma, and P.K. Saini, "Vibration model to detect local defect characteristics of deep groove ball bearing," *Evergreen*, **9** (*4*) 1056–1066 (2022). doi:10.5109/6625791.
8) A.C. Opia, M.K.A. Hamid, S. Samion, C.A.N. Johnson, A.B. Rahim, and M.B. Abdulrahman, "Nano-particles additives as a promising trend in tribology: a review on their fundamentals and mechanisms on friction and wear reduction," *Evergreen*, **8** (*4*) 777–798 (2021). doi:10.5109/4742121.
9) M.S.H. Ador, S. Kabir, F. Ahmed, F. Ahmad, and S. Adil, "Effects of minimum quantity lubrication (mql) on surface roughness in milling al alloy 383 / adc 12 using nano hybrid cutting fluid," *Evergreen*, **9** (*4*) 1003–1020 (2022). doi:10.5109/6625790.
10) N.K. Yadav, N.S. Rajput, S. Kulshreshtha, and M.K. Gupta, "Investigation of the mechanical and wear properties of epoxy resin composite (ercs) made with nano particle tio2 and cotton fiber reinforcement," *Evergreen*, **10** (*1*) 63–77 (2023). doi:10.5109/6781041.
11) W. Libyawati, G. Kiswanto, A.S. Saragih, and T.J. Ko, "The influence of flexure variation to vibration-assisted micro-milling device by using finite element analysis," *Evergreen*, **9** (*2*) 577–583 (2022). doi:10.5109/4794205.
12) S. Mittal, and V.K. Mittal, "Experimental investigation for tribological properties in mixed regime of lubrication with vg-46 and vg-32.," *Evergreen*, **9** (*3*) 694–700 (2022). doi:10.5109/4843100.
13) S. Mittal, and V.K. Mittal, "The effect of hardness of base material on tribological properties of vg-46 lubricant in mixed lubrication regime," *Evergreen*, **10** (*3*) 1366–1373 (2023). doi:10.5109/7151684.
14) A. Aziz, M. Azka, N.C. Majid, M. Al Huda, A. Susanto, K. Jauhari, A.Z. Rahman, and R. Nurmayni, "Influence of lubrication on vibration response and surface roughness in milling of aluminum 6061," *Evergreen*, **10** (*3*) 1762–1769 (2023). doi:10.5109/7151725.
15) V.A. Gandhari, M.S. Perdani, and H. Hermansyah, "Improvement on reusability, storage stability and thermal stability of magnetic graphene oxide-immobilized cholesterol oxidase," *Evergreen*, **9** (*2*) 500–505 (2022). doi:10.5109/4794178.
16) K. Uddin, I.I. El-Sharkawy, T. Miyazaki, B.B. Saha, and S. Koyama, "Thermodynamic analysis of adsorption cooling cycle using ethanol-surface treated maxsorb iii pairs," *Evergreen*, **1** (*1*) 25–31 (2014). doi:10.5109/1440973.
17) A. Yousefian, and N. Yamamoto, "3D finite difference time domain simulation of microwave propagation in a coaxial cable," *Evergreen*, **5** (*3*) 1–11 (2018). doi:10.5109/1957495.
18) A. Dhiman, and G. Sachdeva, "Energy and exergy analysis of a pressurized solar cooking system based on a parabolic dish collector," **09** (*04*) 1168–1180 (2022).
19) T. Negi, H. Mizunaga, and T. Uchida, "A technique for calculating magnetotelluric impedance based on the presence of noise," *J. Nov. Carbon Resour. Sci.*, **6** (*1*) 36–40 (2012).
20) G. Burshukova, A. Kanazhanov, R. Abuova, and A. Joldassov, "Analysis of using damping alloys to improve vibration and strength characteristics in the automotive industry," *Evergreen*, **10** (*2*) 742–751 (2023). doi:10.5109/6792824.
21) R. Yoneda, "Research and technical trend in nuclear fusion in japan," *Evergreen*, **4** (*4*) 16–23 (2017). doi:10.5109/1929677.
22) N.Z. Zaini, N.B. Kamaruzaman, and U. Abidin, "Magnetic microbeads trapping using microfluidic and permanent magnet system," *Evergreen*, **8** (*1*) 156–162 (2021). doi:10.5109/4372272.
23) Monica Niken Aprilliani, B. Rusdiarso, and W. Trisunaryanti, "Synthesis of activated carbon-fe_3o_4 composite as gasoline adsorbent in gasoline-water mixture and its adsorption kinetics study," *Evergreen*, **9** (*3*) 701–710 (2022). doi:10.5109/4843101.
24) Y.C. Wu, W.T. Tseng, and Y.T. Chen, "Torque ripple suppression in an external-meshed magnetic gear train," *Adv. Mech. Eng.*, **2013** (2013). doi:10.1155/2013/178909.
25) G. Muruganandam, S. Padma, and P. Selvakumar, "Torque analysis of magnetic spur gear with different configurations," *Int. J. Electr. Eng.*, **5** (*7*) 843–852 (2012). http://www.irphouse.com.
26) E.P. Furlani, "Analytical analysis of magnetically coupled multipole cylinders," *J. Phys. D. Appl. Phys.*, **33** (*1*) 28–33 (2000). doi:10.1088/0022-3727/33/1/305.
27) F. Jorgensen, and T. Andersen, "Two dimmensional model of a permanent magnet spur gear," *Conf. Rec. 2005 IEEE Ind. Appl. Conf.*, **1–4** 261–265 (2005). http://scholar.google.com/scholar?hl=en&btnG=Search&q=intitle:Two+dimmensional+model+of+a+permanent+magnet+spur+gear+-+A+mathematical+method+used+to+model+a+parallel+magnetised+magnetic+spur+gear#1.
28) Y.C. Wu, and C.W. Wang, "Transmitted torque analysis of a magnetic gear mechanism with rectangular magnets," *Appl. Math. Inf. Sci.*, **9** (*2*) 1059–1065 (2015). doi:10.12785/amis/090257.
29) T.K. Bang, K.H. Shin, M.M. Koo, C. Han, H.W. Cho, and J.Y. Choi, "Measurement and torque calculation

of magnetic spur gear based on quasi 3-d analytical method," *IEEE Trans. Appl. Supercond.*, **28** (*3*) (2018). doi:10.1109/TASC.2017.2779750.

30) Y.R. Vishnu, M. Nair, L.K. Varghese, M. Vincent, and D. Wilson, "Magnetic gearing system," *IJIRST – International J. Innov. Res. Sci. Technol.*, **2** (*12*) 11–18 (2016).
31) D.H. K. Atallah, S.D. Calverley, "Design, analysis and realisation of a high_performance magnetic gear," *IEE Proc. - Electr. Power Appl.*, **151** (*2*) 135–143 (2004). doi:10.1049/ip-epa:20040224.
32) M. Desvaux, R.L.G. Latimier, B. Multon, H. Ben Ahmed, and S. Sire, "Design and optimization of magnetic gears with arrangement and mechanical constraints for wind turbine applications," *2016 11th Int. Conf. Ecol. Veh. Renew. Energies, EVER 2016*, (2016). doi:10.1109/EVER.2016.7476341.
33) Y.C. Wu, and B.S. Jian, "Magnetic field analysis of a coaxial magnetic gear mechanism by two-dimensional equivalent magnetic circuit network method and finite-element method," *Appl. Math. Model.*, **39** (*19*) 5746–5758 (2015). doi:10.1016/j.apm.2014.11.058.
34) S.N. Fajri, "Effects of design parameters on the transmitted torque of a coaxial magnetic gear with halbach permanent-magnet array," (*Eic 2018*) 36–42 (2020). doi:10.5220/0009006000360042.
35) X. Liu, K.T. Chau, J.Z. Jiang, and C. Yu, "Design and analysis of interior-magnet outer-rotor concentric magnetic gears," *J. Appl. Phys.*, **105** (*7*) 103–106 (2009). doi:10.1063/1.3058619.
36) M. Fukuoka, K. Nakamura, and O. Ichinokura, "Experimental tests and efficiency improvement of surface permanent magnet magnetic gear," *IEEJ J. Ind. Appl.*, **3** (*1*) 62–67 (2014). doi:10.1541/ieejjia.3.62.
37) M. Desvaux, M. Chauwin, B. Multon, S. Sire, and H. Ben Ahmed, "Experimental validation of a transverse flux magnetic gear," *J. Magn. Magn. Mater.*, **536** (*May*) 1–7 (2021). doi:10.1016/j.jmmm.2021.168139.
38) F.T. Jørgensen, T.O. Andersen, and P.O. Rasmussen, "The cycloid permanent magnetic gear," *IEEE Trans. Ind. Appl.*, **44** (*6*) 1659–1665 (2008). doi:10.1109/TIA.2008.2006295.
39) M.C. Johnson, "Design and analysis of axial and radial flux magnetic gears and magnetically geared machines," (*May*) (2017).
40) M. Desvaux, B. Multon, H. Ben Ahmed, and S. Sire, "Preface," *Mech. Mach. Sci.*, **54** (*February*) v–vi (2018). doi:10.1007/978-3-319-67567-1.
41) D.S. Painter, "A comparative study of the performance capabilities of magnetic gears," (2016).
42) D. Fodorean, "State of the art of magnetic gears, their design, and characteristics with respect to ev application," *Model. Simul. Electr. Veh. Appl.*, (2016). doi:10.5772/64174.
43) R.A. Jessam, "Experimental study of wind turbine power generation utilizing discharged air of air conditioner blower," **09** (*04*) 1103–1109 (2022).
44) I. Tarimer, and C. Ocak, "Performance comparision of internal and external rotor structured wind generators mounted from same permanent magnets on same geometry," *Elektron. Ir Elektrotechnika*, (*4*) 65–70 (2009).
45) J. Wang, L. Qian, S. Xu, and R. Mo, "Analysis of electromagnetic performance of modulated coaxial magnetic gears used in semi-direct drive wind turbines," *Energy Eng. J. Assoc. Energy Eng.*, **118** (*2*) 251–264 (2021). doi:10.32604/EE.2021.014143.